의학박사 학위 논문

Inter-strain Comparison of Rodent Glaucoma Models: Magnetic Bead Injection Versus Hydrogel Injection Versus Circumlimbal Suture

설치류 녹내장 모델의 동물 주간 비교

2023년 8월

서울대학교 대학원

의학과 안과학 전공

이 경 민

Inter-strain Comparison of Rodent Glaucoma Models: Magnetic Bead Injection Versus Hydrogel Injection Versus Circumlimbal Suture

설치류 녹내장 모델의 동물 주간 비교

지도 교수 김 태 우

이 논문을 의학 박사 학위논문으로 제출함
2023년 4월

서울대학교 대학원
의학과 안과학 전공
이 경 민

이경민의 의학 박사 학위논문을 인준함
2023년 7월

위 원 장 구 자 원 (인)

부위원장 김 태 우 (인)

위 원 정 진 행 (인)

위 원 이 은 지 (인)

위 원 성 경 림 (인)

ABSTRACT

Purpose: To compare the inter-strain differences of three rodent glaucoma models as induced by magnetic bead injection, hydrogel injection, and circumlimbal suture.

Methods: In Brown-Norway (BN) and Sprague-Dawley (SD) rat strains, intraocular pressure (IOP) was elevated by injection of magnetic beads or hydrogel to obstruct the aqueous humor outflow or by external compression of circumlimbal suture. Maximum and average IOP values were compared according to both procedure and rat strain over one month postoperatively. Retinal ganglion cell (RGC) density loss was evaluated using confocal microscopic images of the flat-mounted retina obtained at postoperative day 14 and 30.

Results: The IOP profiles showed steady increase for the magnetic bead injection model, IOP spikes followed by gradual decrease for the hydrogel injection model, and IOP spikes followed by sudden decrease for the circumlimbal suture model. The maximum IOPs were higher in the hydrogel injection or circumlimbal injection models than in the magnetic bead injection model ($P < 0.001$), while average IOP showed no difference between the two strains (both $P \geq 0.05$). A generalized estimating equation regression model showed that IOP increase was maintained better in the BN rats than in the SD rats ($P < 0.001$). Such inter-strain difference was smaller in the circumlimbal suture model. Significant RGC-density decrease was observed in all of the models for the BN rats and in the circumlimbal suture model for the SD rats at postoperative day 30.

Conclusions: BN rats were advantageous for the magnetic bead or hydrogel

injection model, while either rat strain could be used for the circumlimbal suture model. Strains should be considered cautiously when establishing rodent glaucoma models of varying nature and IOP profiles.

Keywords: Rodent glaucoma model; magnetic bead; hydrogel; circumlimbal suture; retinal ganglion cell; intraocular pressure

Student Number: 2016-30587

CONTENTS

LIST OF TABLES AND FIGURES

LIST OF ABBREVIATIONS

BN: Brown-Norway

GEE: generalized estimating equation

HCCS: HyStem Cell Culture Scaffold

IOP: intraocular pressure

SD: Sprague-Dawley

RGC: retinal ganglion cell

INTRODUCTION

Glaucoma is the leading cause of irreversible blindness in the world,[1] and its prevalence is expected to increase steadily.[2, 3] Glaucoma's characteristic feature is progressive axonal loss of retinal ganglion cells (RGCs), but its detailed pathophysiology has yet to be fully explained.[4] Many factors such as mechanical, ischemic, metabolic, and immunologic insults have been nominated as candidate sources of axonal damage,[4-7] while intraocular pressure (IOP) is the only controllable factor in practice.

To understand the pathogenesis of glaucoma and to improve its therapy, various glaucoma animal models have been developed with many species including monkeys,[8-11] dogs,[12] and rodents (mice/rats).[13-38] Once a glaucoma animal model, as characterized by progressive RGC loss associated with IOP elevation, is established, various glaucoma treatment modalities can be tested in preclinical trials. For that reason, glaucoma animal models are designed to have inducibly or spontaneously increased IOP. Among them, rodent glaucoma models are frequently used due to ease and low cost of implementation. Most currently available rodent models are accomplished by laser treatment of the outflow area,[13-15] cautery or affliction of osmotic damage to the episcleral and vortex veins,[16, 17] external ocular compression using circumlimbal suture,[18-20] or injection of beads[21-28] or hydrogel[33-38] into the anterior chamber.

Each rodent glaucoma model, however, is established based on a different rat strain,[28] and strains are reported to have different IOP and RGC death profiles.[22, 26] Therefore, in order to improve the efficiency of any rodent glaucoma model, inter-

strain comparison is necessary. The purpose of the present study was to compare three rodent glaucoma models — 1) magnetic bead injection model, 2) hydrogel injection model, 3) circumlimbal suture model — against two different rat strains (Brown-Norway [BN], Sprague-Dawley [SD]). This comparison will enable the use of the most effective strain for each model, and thereby, it will facilitate the better use of rodent glaucoma models for disease and treatment discovery and testing.

MATERIALS AND METHODS

Animals

This study was conducted in accordance with the Association for Research in Vision and Ophthalmology Guide for the Care and Use of Laboratory Animals, using protocols approved and monitored by the Seoul National University Boramae Medical Center Institutional Animal Care and Use Committee (No. 2021-0023). Seventy (70) male BN rats and 50 male SD rats aged 8 months each weighing 250–300 g were housed in a constant low-light environment (40–60 lux) to minimize diurnal fluctuations in IOP, with food and water provided ad libitum. All of the surgical procedures were performed under general anesthesia induced by isoflurane inhalation (**Figure 1**).

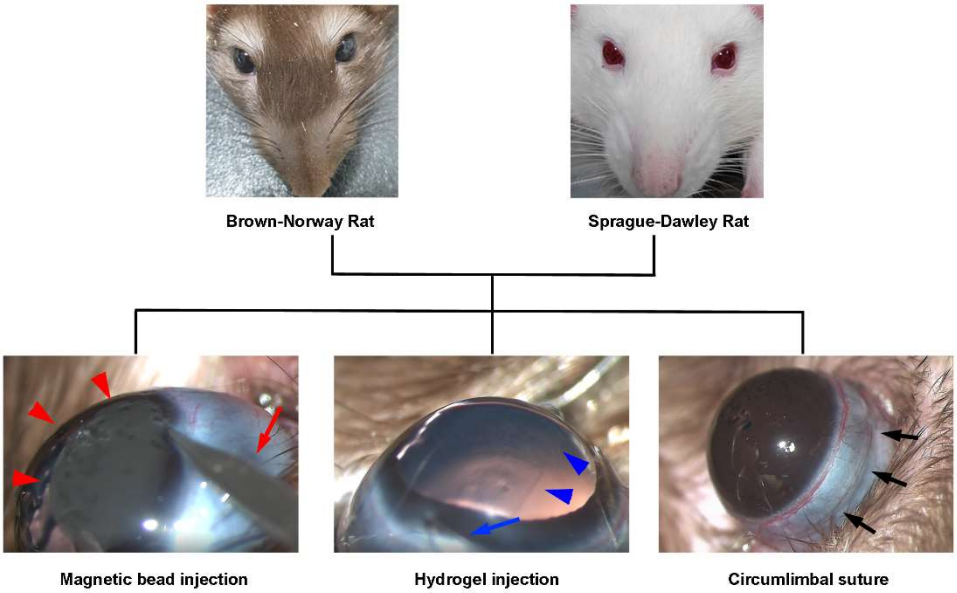

Figure 1. Study design scheme. Brown-Norway and Sprague-Dawley rats were compared for three rodent glaucoma models. Aqueous humor outflow was obstructed by injection of either magnetic beads (red arrowheads) or hydrogel (blue arrowheads). For this purpose, the glass capillary needle was fabricated to have very narrow and sharp tips (red and blue arrows). External pressure was applied by circumlimbal suture 1~1.5mm behind the limbus (black arrows).

Measurement of IOP

IOP was measured three times preoperatively to calculate the baseline, and was again measured immediate-postoperatively, on postoperative day 1, postoperative day 2, and every 3 to 4 days up to one month after injection using a rebound tonometer (Tonolab, Icare®, Finland) specifically calibrated for use with the rat eye.[39] All measurements were made in awake animals under topical anesthesia induced by 0.5% proparacaine hydrochloride eye drops (Hanmi Pharm. Co., Seoul, Korea). IOP was measured five times for a single measurement, and the mean of those values was calculated after excluding the highest and lowest results and subsequently used in the analysis. Besides individual IOP values, two representative values were investigated: 1) maximum IOP value during follow-up, and 2) average integral IOP, defined as the area under the IOP curve[38, 40] divided by the observed days for each subject.

Induction of ocular hypertension

1. Preparation of injection set-up

A glass micropipette for ocular injection was made by pulling a glass capillary tube (1.0/0.75 mm outer /inner diameter) with a micropuller (PC-100; Narishige, Tokyo, Japan). One of the tips of the tube was broken and ground using a microgrinder (EG-401; Narishige) to a final diameter of approximately 100 μm.[23] After filling the glass capillary tube with injection materials (magnetic bead or hydrogel), the tube was connected to a pneumatic microinjector (IM-11-2; Narishige) for application of positive continuous pressure to facilitate full delivery throughout the injection with no dead spaces (**Figure 2**).

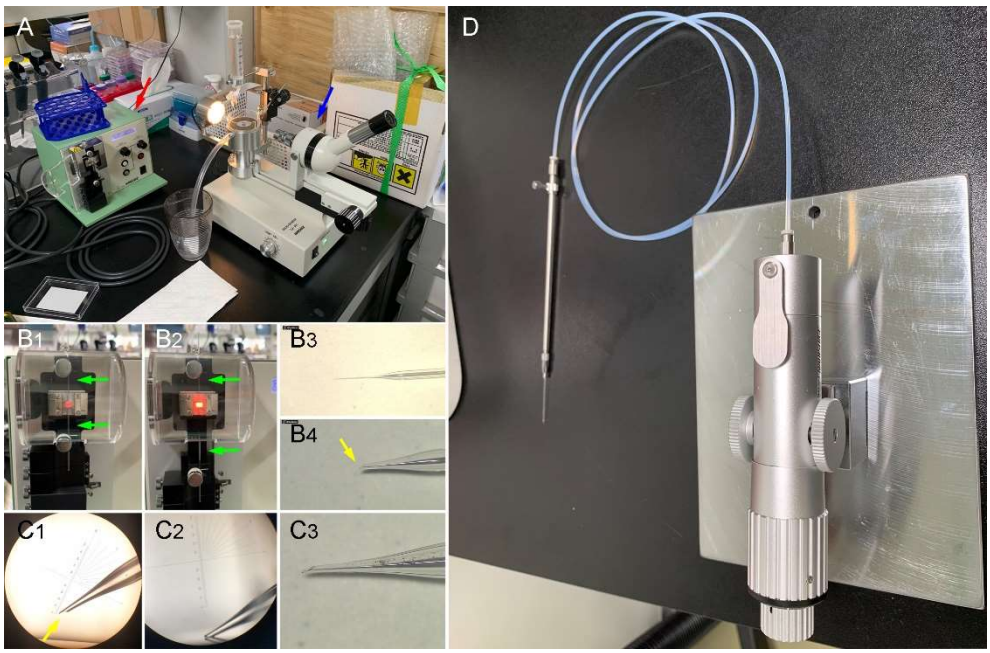

Figure 2. Preparation of injection set up. (**A**) Preparation of a glass micropipette with a micropuller (red arrow) and a microgrinder (blue arrow). (**B**) The micropuller pulls a glass capillary needle (**B_{1-2}**, between green arrows), which produces a very sharp needle (**B_3**). Then, the needle is broken to widen its internal lumen (**B_4**, yellow arrow). (**C_{1-2}**) The microgrinder grinds the broken needle to produce a fine micropipette with bevel (**C_3**). (**D**) The pneumatic microinjector enables injection without creating dead space.

2. Magnetic bead injection

Twenty-six (26) BN rats and 17 SD rats were subjected to magnetic bead injection. Magnetic beads were prepared at the concentration of 15 mg carboxyl ferro-magnetic microspheres per mL, mixing intermediate size (8.0–8.9 μm diameter; CFM-80-5; Spherotech, Lake Forest, Illinois, USA) with small size (4.0–4.9 μm diameter; CFM-40-10; Spherotech, Lake Forest) microspheres at a 2:1 ratio.[41, 42] The inside of the glass capillary tube was filled with 10 μl of magnetic beads solution using a Hamilton syringe. The empty space of the tube in the tail was filled with viscoelastic material (DisCoVisc; Alcon, Fort Worth, TX, USA). In each procedure, the magnetic beads solution and viscoelastic material were injected into the anterior chamber through a tunnel located near and parallel to the limbus. After injection, a handheld magnet was applied to the side opposite to the injection to prevent reflux spillage of magnetic beads through the incision tunnel (**Figure 3**).[25, 29, 32]

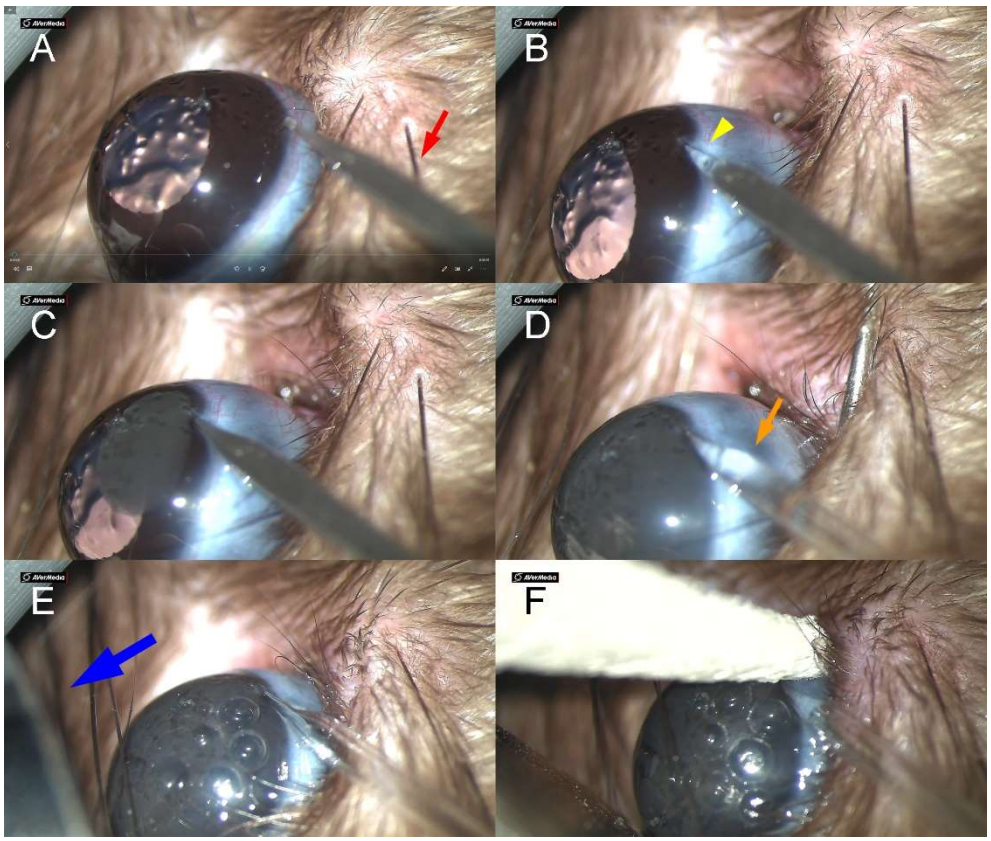

Figure 3. Magnetic bead injection. (**A**) While an eyeball is exposed and supported by McPherson forceps (invisible), a micropipette filled with magnetic beads is positioned (red arrow). (**B**) An injection is performed parallel to the limbus to prevent reflux spillage, but reflux of aqueous humor (yellow arrowhead) is visible immediately after the micropipette reaches the anterior chamber, due to intraocular pressure elevation that occurs while exposing the eyeball. (**C**) Spreading of magnetic beads into the anterior chamber with injection. (**D**) Viscoelastic material (orange arrow) in the tail of the micropipette to prevent magnetic bead attachment to corneal endothelium (DisCoVisc; Alcon, Fort Worth, TX, USA). (**E**) At the end of injection, a magnet (blue arrow) is applied to the side opposite to the injection to prevent reflux spillage of the magnetic beads. (**F**) While holding the magnet, the

needle is removed safely.

3. Hydrogel injection

Twenty-six BN (26) rats and 17 SD-rats were subjected to hydrogel injection. For this purpose, a pre-mixed *in situ* cross-linking hydrogel (HyStem Cell Culture Scaffold [HCCS] kit; Sigma-Aldrich, St. Louis, MO, USA) was injected into the anterior chamber in the same manner as reported previously.[34, 37] The HCCS kit consisted of HyStem (thiol-modified carboxymethyl hyaluronic acid) and Extralink (thiol-reactive polyethylene glycol diacrylate), both dissolved in degassed water according to the manufacturer's instruction and mixed at the ratio of 4:1 immediately before injection.[34, 37] The inside of the glass capillary tube was filled with 10 µl of HCCS using, as in the magnetic bead injection model, a Hamilton syringe. The empty space of the tube in the tail was filled, consistently again with the magnetic bead injection model, with viscoelastic material (DisCoVisc). In each procedure, the HCCS and viscoelastic material were injected into the anterior chamber through a tunnel located near and parallel to the limbus (**Figure 4**).

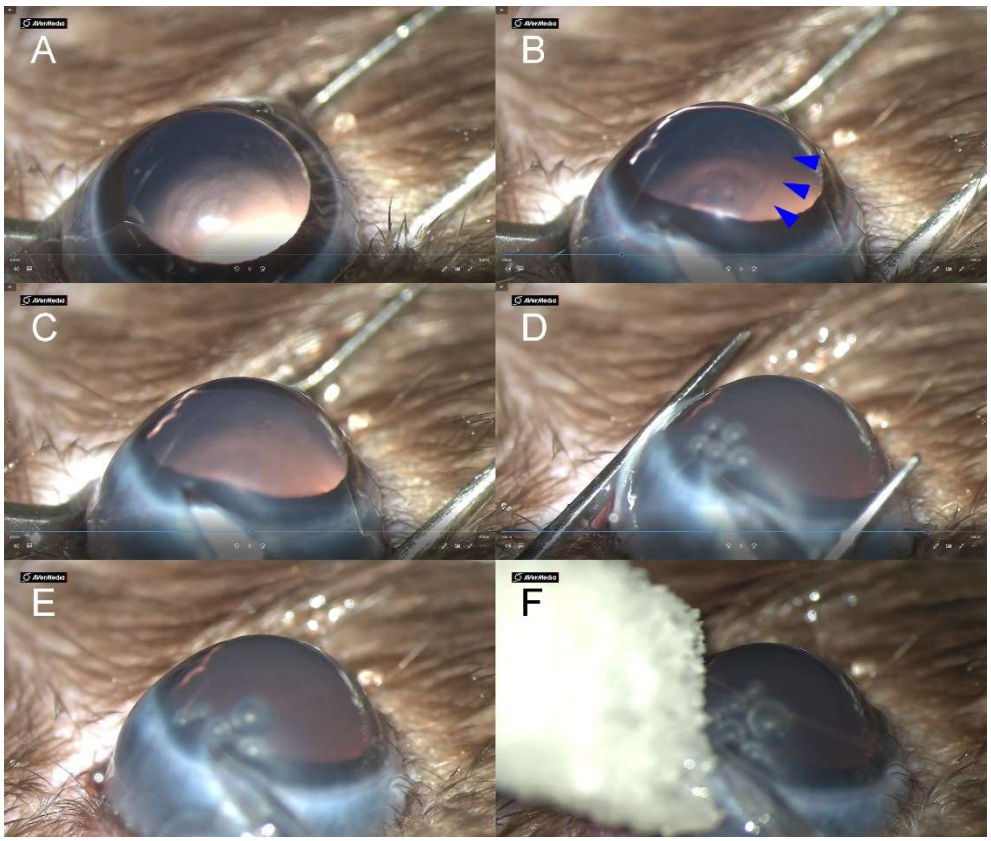

Figure 4. Hydrogel injection. (**A**) An eyeball is exposed and supported by McPherson forceps. (**B**) An injection is performed parallel to the limbus, and spreading of hydrogel into the anterior chamber is visible at the beginning (blue arrowheads). (**C**) Later, the boundary between the hydrogel and aqueous humor becomes indiscernible. (**D**–**F**) After injection, the McPherson forceps and needle are removed sequentially.

4. Circumlimbal suture

Eighteen (18) BN rats and 16 SD rats were subjected to circumlimbal suturing. The suturing was performed around the globe approximately 1.0–1.5 mm behind the limbus using 7/0 nylon to pressurize the eyeball as in previous reports (**Figure 5**).[18-20]

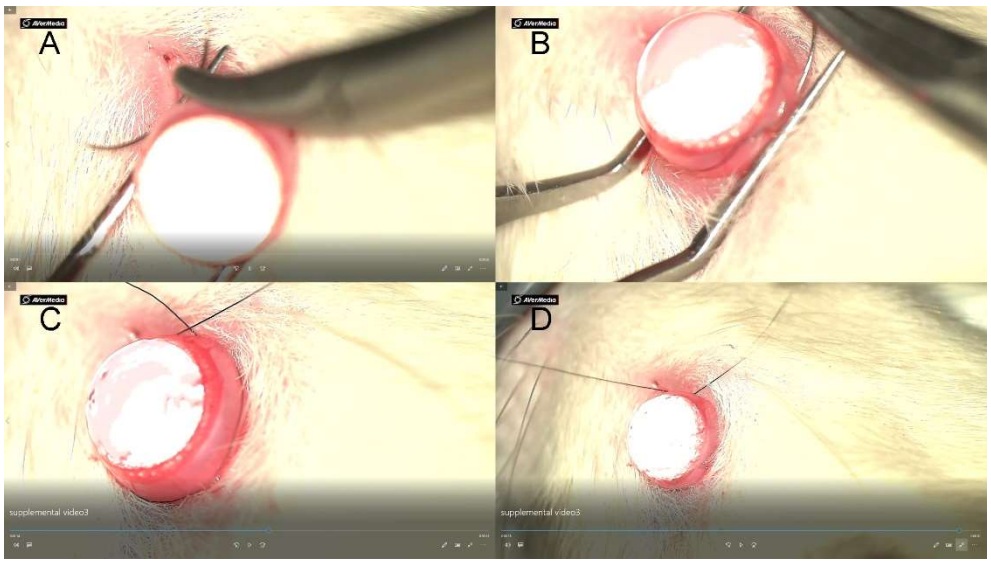

Figure 5. Circumlimbal suture. (**A**) While an eyeball is exposed and supported by McPherson forceps, 7/0 nylon suture is applied 1.0–1.5 mm behind the limbus. (**B**–**C**) An average of five sutures are made while avoiding damage to the limbal vessels. (**D**) The circumferential suture is tightened up to pressurize the eyeball.

RGC counts

To determine the number of RGCs, the rats were heavily anesthetized on day 14 and 30 by isoflurane inhalation and euthanized in a CO_2 chamber, affording at least 5 samples for each time point of the glaucoma model. For comparison, 5 additional samples were obtained from healthy subjects for each strain. Eyes were immediately enucleated and fixed with 10% neutral buffered formalin (NBF) for 4 minutes at room temperature. After that, the retina was dissected, flattened with four radial cuts, the vitreous removed, and the retina flat-mounted, RGC layer up, on a glass slide. The retinas were labeled with RGC-targeting anti-Brn3a antibody (sc-8429; Santa Cruz, Dallas, TX, USA) and counterstained with 4',6-diamidino-2-phenylindole (DAPI; D9542, Sigma-Aldrich). Then, the retinas, still flat-mounted, were imaged by confocal microscopy (Leica STELLARIS 8, Wetzlar, Germany) for quantification of RGC densities. A total of 36 images for each eye (3 spots for each 1, 2 and 3mm areas from the optic nerve head in four quadrants) were obtained (200× magnification, 0.31 μm/pixel). RGCs were counted by the automated cell-counting software developed by Guymer and Damp et al.[43]

Statistical analysis

All statistical analyses were performed with commercially available software (Stata version 16.0; StataCorp, College Station, TX, USA) and R statistical packages version 4.1.2 (available at http://www.r-project.org; assessed November 1, 2021). A generalized estimating equation (GEE) regression model was applied to simulate the IOP change over time according to the glaucoma model and strain. RGC density was compared by Kruskal-Wallis testing. The data herein are presented as

mean ± standard deviations except where stated otherwise; the cutoff for statistical significance had been set to $P < 0.05$.

To calculate the required sample size, we anticipated that the IOP would be, at minimum, more than 25 *mmHg* after each procedure relative to the IOP of 10 *mmHg* in the fellow control eye. When a standardized mean difference was assumed as 25 *mmHg*, a sample of 24 subjects was required to detect the difference in IOP with 80% power using a 2-sided 5%-level paired *t*-test. Since half of the subjects were to be sacrificed after two weeks to obtain the RGC density data, a total 48 subjects were required to detect the differences in the IOPs throughout the entire period.

RESULTS

IOP elevation profile

Following the surgical procedures, the IOP increased and then slowly decreased with time in all cases (**Figure 6**). The IOP increase patterns, however, differed among the procedures: 1) the magnetic bead injection model induced a gradual increase of IOP; 2) the hydrogel injection model induced a spike immediate-postoperatively with gradual decrease of IOP thereafter, and 3) the circumlimbal suture model induced an immediate-postoperative spike with rapid decrease of IOP thereafter (**Figure 6**). The maximum IOP was higher in the hydrogel injection and circumlimbal suture models than in the magnetic bead injection model, while the average integral IOP showed no difference among the models (**Table 1**).

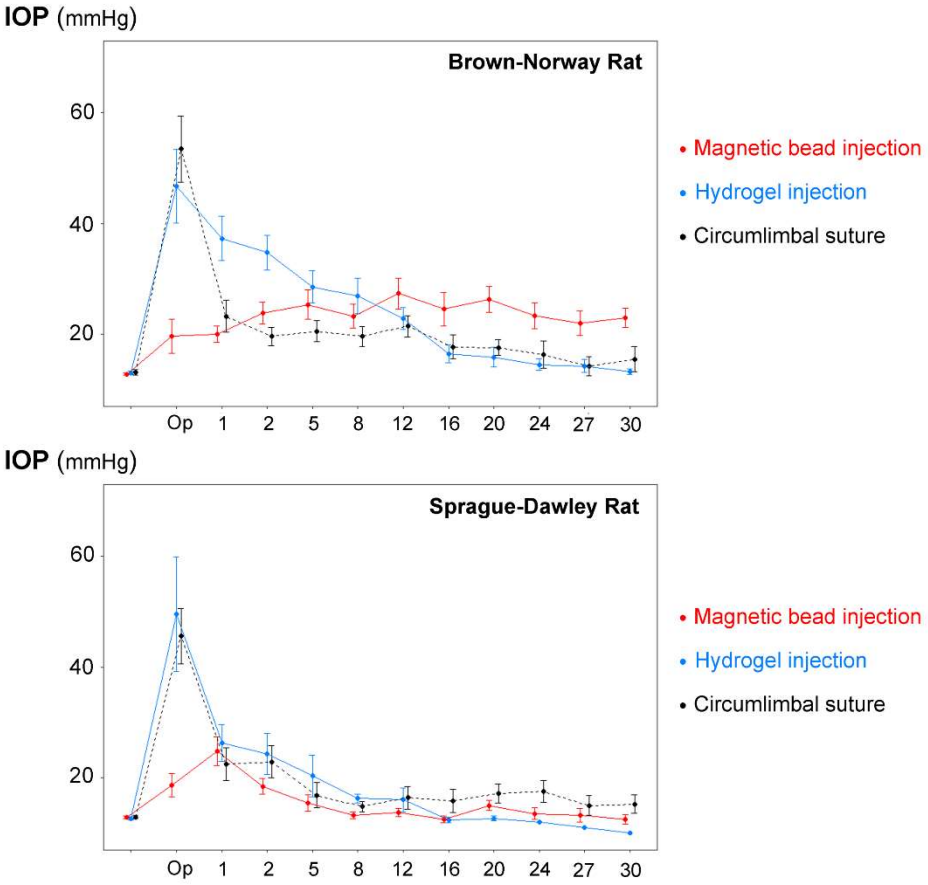

Figure 6. Intraocular pressure (IOP) profiles according to strains and rodent glaucoma models. Magnetic bead injection model induced gradual increase of IOP. Hydrogel injection model induced immediate IOP followed by gradual decrease of IOP. Circumlimbal suture model induced immediate IOP spike followed by rapid decrease of IOP. Magnetic bead and hydrogel injection models maintained IOP increase of IOP longer in Brown-Norway rats than in Sprague-Dawely rats. Bars indicate 95% confidence interval.

Table 1. Demographics and intraocular pressure (IOP) profiles of each group

IOP parameters	Magnetic bead injection (A)	Hydrogel injection (B)	Circumlimbal suture (C)	P^*	*Post-hoc analysis*
Brown-Norway rat, *numbers*	26	26	18		
Baseline IOP, *mmHg*	12.8 ± 0.8	13.0 ± 1.2	13.1 ± 1.6	0.714	
Maximum IOP, *mmHg*	34.3 ± 14.6	53.8 ± 15.8	54.3 ± 18.3	<0.001	A < B = C
Average Integral IOP, *mmHg*	24.7 ± 8.5	27.0 ± 12.8	25.9 ± 10.5	0.782	
Sprague-Dawley rat, *numbers*	17	17	16		
Baseline IOP, *mmHg*	12.9 ± 0.9	12.7 ± 0.7	12.9 ± 0.9	0.828	
Maximum IOP, *mmHg*	25.6 ± 9.5	50.7 ± 19.8	45.9 ± 14.5	<0.001	A < B = C
Average Integral IOP, *mmHg*	16.3 ± 4.1	21.3 ± 12.0	25.7 ± 11.8	0.059	

*Comparison performed using one-way ANOVA test with post-hoc Scheffe analysis

In the BN rats, after magnetic bead injection, 26 (100%) had a maximum IOP over 20 *mmHg* and 20 (77%) had an average integral IOP over 20 *mmHg*; after hydrogel injection, 25 (96%) had a maximum IOP over 20 *mmHg* and 20 (77%) had an average integral IOP over 20 *mmHg*; after circumlimbal suture, 18 (100%) had a maximum IOP over 20 *mmHg* and 14 (78%) had an average integral IOP over 20 *mmHg*.

In the SD rats after magnetic bead injection, 13 (76%) had a maximum IOP over 20 *mmHg* and 4 (24%) had an average integral IOP over 20 *mmHg*; 11 (65%) had a maximum IOP over 20 *mmHg* and 6 (35%) had an average integral IOP over 20 *mmHg*; after circumlimbal suture, 16 (100%) had a maximum IOP over 20 *mmHg* and 13 (81%) had an average integral IOP over 20 *mmHg*.

The constructed GEE regression model evaluated the effects of each procedure and strain on the IOP profile (**Table 2**). Increased IOP was slowly normalized as time passed. The hydrogel injection and the circumlimbal suture models induced more abrupt IOP increases (both $P < 0.001$) than did the magnetic bead injection model. The SD rat strain showed lesser IOP elevation ($P < 0.001$) than did the BN rat strain.

Table 2. Intraocular pressure according to postoperative day, glaucoma animal model, and strain

	Generalized estimating equation regression model			
	Coefficient	Standard error	95% confidence interval	*P*
Postoperative day	0.069	0.036	(-0.002, 0.140)	0.056
Glaucoma model (vs. Magnetic bead injection)				
Hydrogel injection	**13.406**	**0.847**	**(11.745, 15.067)**	**< 0.001**
Circumlimbal suture	**13.658**	**0.771**	**(12.148, 15.169)**	**< 0.001**
Strain (vs. Brown-Norway rat)				
Sprague-Dawley rat	**-2.755**	**0.671**	**(-4.070, -1.439)**	**< 0.001**

Statistically significant values ($P < 0.05$) are shown in bold.

Differences among glaucoma models

Eye enlargement (buphthalmos) was observed in all of the BN-rats of the magnetic bead injection model (**Figure 7A$_{1–2}$**, red arrows), but in 4 (15%) of the BN rats of the hydrogel injection model (**Figure 7A$_3$**, blue arrow) and in 1 (6%) of the SD rats of the magnetic bead injection model (**Figure 7A$_4$**, orange arrow). Three (3) of the 26 eyes (12%) of the magnetic-bead-injected BN rats developed hyphema as a consequence of neovascular complication, and thus were excluded from the analysis (**Figure 7B$_{1-2}$**, red arrow). No neovascular complications were not observed in either the hydrogel injection or circumlimbal suture model.

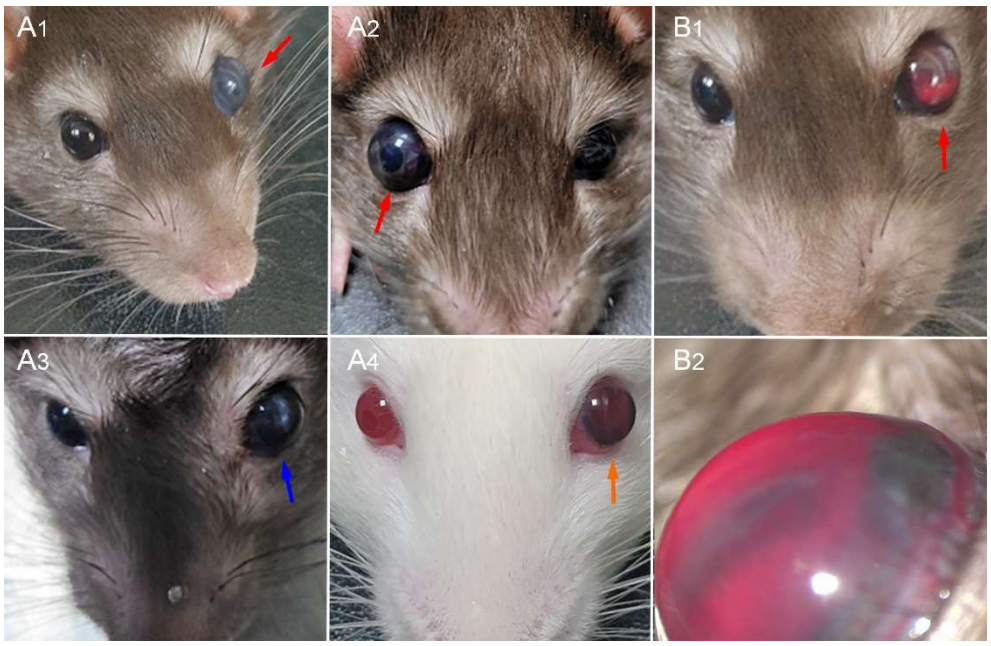

Figure 7. Gross anatomic changes. (**A**) Buphthalmos in magnetic bead injection model of Brown-Norway rats (**$A_{1–2}$**, red arrows), in hydrogel injection model of Brown-Norway rats (**A_3**, blue arrow), and in the magnetic bead injection model of Sprague-Dawley rats (**A_4**, orange arrow). These changes were not observed in the circumlimbal suture model. (**B**) Neovascular complication after magnetic bead injection model (**B_1**, red arrow). These changes were not observed in either the hydrogel injection model or the circumlimbal suture model.

RGC comparison

For the BN rats, the average RGC density (cell counts/mm^2) was 1886 ± 456, which had decreased to 1485 ± 418 (78.7 ± 22.2%) at day 14 and 1145 ± 506 (60.7 ± 26.8%) at day 30 post-magnetic bead injection ($P < 0.001$). After hydrogel injection, the RGC density decreased to 1662 ± 479 (88.1 ± 25.4%) at day 14 and 1346 ± 688 (71.4 ± 36.5%) at day 30 ($P < 0.001$). After circumlimbal suture, the RGC density decreased to 1791 ± 506 (95.0 ± 26.8%) at day 14 and 1413 ± 519 (74.9 ± 27.5%) at day 30 ($P = 0.028$, **Table 3**) (**Figure 8** & **Figure 9A–D**).

For the SD-rats, the average RGC density (cell counts/mm^2) was 1872 ± 210, which had decreased to 1703 ± 617 (91.0 ± 33.0%) at day 14, 1694 ± 430 (90.5 ± 22.9%) at day 30 post-magnetic bead injection ($P = 0.425$). After hydrogel injection, the RGC density decreased to 1706 ± 416 (91.1 ± 22.2%) at day 14 and 1683 ± 446 (89.9 ± 23.8%) at day 30 ($P = 0.489$). After circumlimbal suture, the RGC density decreased to 1734 ± 494 (92.6 ± 26.4%) at day 14 and 1456 ± 432 (77.8 ± 23.1%) at day 30 ($P < 0.001$, **Table 3**) (**Figure 8** & **Figure 9E–H**).

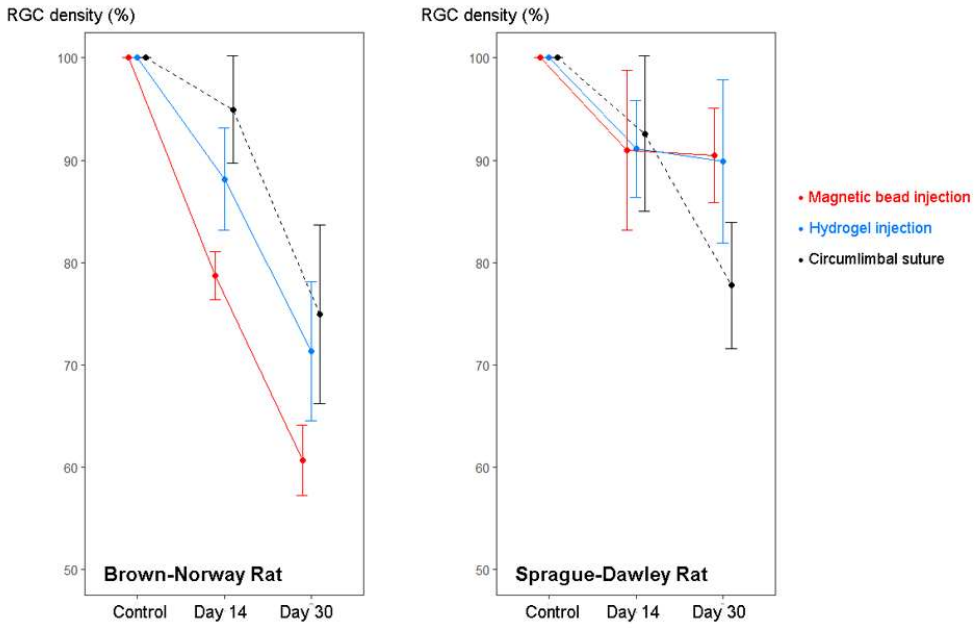

Figure 8. Retinal ganglion cell (RGC) density percentage changes from baseline according to strains and rodent glaucoma models. From the flat-mounted retina, a total of 36 images for each eye (3 spots for each 1, 2 and 3mm areas from the optic nerve head in four quadrants) were obtained, and the average values were used in the analysis. In both Brown-Norway and Sprague-Dawley rats, RGC density decrease was observed in the following order: magnetic bead injection model, hydrogel injection model, circumlimbal suture model. Bars indicate 95% confidence interval.

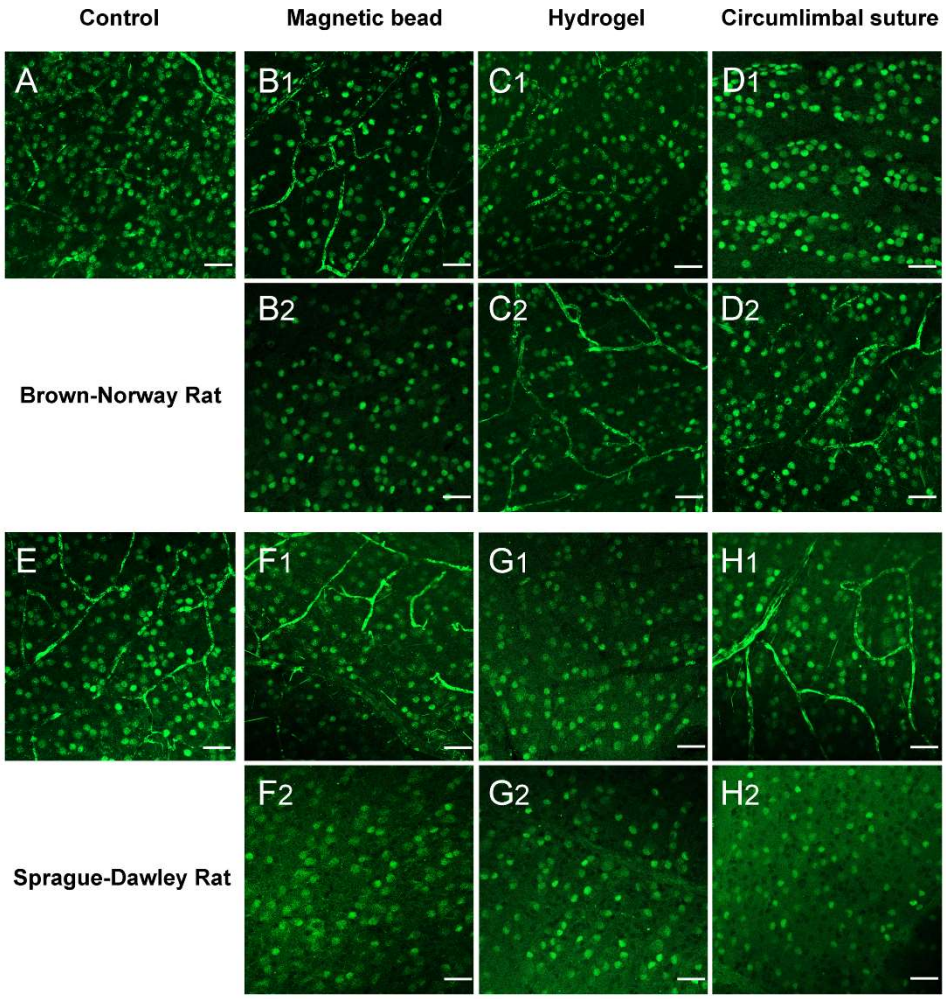

Figure 9. Brn3a-stained retinal ganglion cells. (Scale bar: 20μm). (**A**–**D**) Brown-Norway rats. (**A**) Control. (**B**) Magnetic bead injection model at day 14 ($\mathbf{B_1}$) and day 30 ($\mathbf{B_2}$). (**C**) Hydrogel injection model at day 14 ($\mathbf{C_1}$) and day 30 ($\mathbf{C_2}$). (**D**) Circumlimbal suture model at day 14 ($\mathbf{D_1}$) and day 30 ($\mathbf{D_2}$). (**E**–**H**) Sprague-Dawley rats. (**E**) Control. (**F**) Magnetic bead injection model at day 14 ($\mathbf{F_1}$) and day 30 ($\mathbf{F_2}$). (**G**) Hydrogel injection model at day 14 ($\mathbf{G_1}$) and day 30 ($\mathbf{G_2}$). (**H**) Circumlimbal suture model at day 14 ($\mathbf{H_1}$) and day 30 ($\mathbf{H_2}$).

Table 3. Retinal ganglion cell density changes according to glaucoma animal model and strain

Cell counts/mm^2	Magnetic bead injection	Hydrogel injection	Circumlimbal suture	*P* (over models)
Brown-Norway rat (Control)		1886 ± 456		
Day 14	1485 ± 418	1662 ± 479	1791 ± 506	0.011*
Day 30	1145 ± 506	1346 ± 688	1413 ± 519	0.304*
P (over weeks)	<0.001*	<0.001*	0.028*	
Sprague-Dawley rat (Control)		1872 ± 210		
Day 14	1703 ± 617	1706 ± 416	1734 ± 494	0.945*
Day 30	1694 ± 430	1683 ± 446	1456 ± 432	0.181*
P (over weeks)	0.425*	0.489*	<0.001*	

*Comparison performed using Kruskal-Wallis test.

DISCUSSION

In this study, we compared three inducible rodent glaucoma models against two different rat strains. Ocular hypertension was induced by either internal blockage of aqueous humor outflow (with magnetic bead or hydrogel injection) or by external compression with circumlimbal suture, which latter mode is thought to render aqueous humor overflow excessive of drainage capacity.[18] With both strains, the magnetic bead injection model resulted in a steady increase of IOP without spikes, while the hydrogel injection model and circumlimbal suture model required an immediate IOP spike to maintain increased IOP for more than 2 weeks. For the internal approach (magnetic bead or hydrogel injection), the BN rats were superior to the SD rats in the aspect of increased-IOP maintenance. No such strain difference was observed for the external approach (i.e., the circumlimbal suture model). This implied that different strains might affect IOP increase differently depending on the model mechanism, and thus should be considered cautiously when establishing any rodent glaucoma model.

The use of magnetic beads has the merit of preventing reflux spillage during needle removal, specifically by means of a magnet that keeps the beads away from the needle track (**Figure 3**). Upon needle removal, the high-pressure gradient between the inside and outside of the eyeball and the patent needle track leads to reflux of the aqueous humor and beads (**Figure 10**). To prevent this, we adopted three strategies: 1) use of a glass capillary needle fabricated to have very narrow and sharp tip, 2) performing of an incision parallel to the corneal limbus to make a longer track, and 3) use of a magnet and magnetic beads to hold the beads at the end of

procedure. By these means, we could prevent spillage of magnetic beads, though aqueous humor reflux could not be completely blocked. The magnetic bead injection model showed a steady increase of IOP without any immediate IOP spike. This absence of IOP spike might be the result of the incomplete blocking of aqueous humor reflux, which presumably neutralized IOP in the immediate-postoperative period.

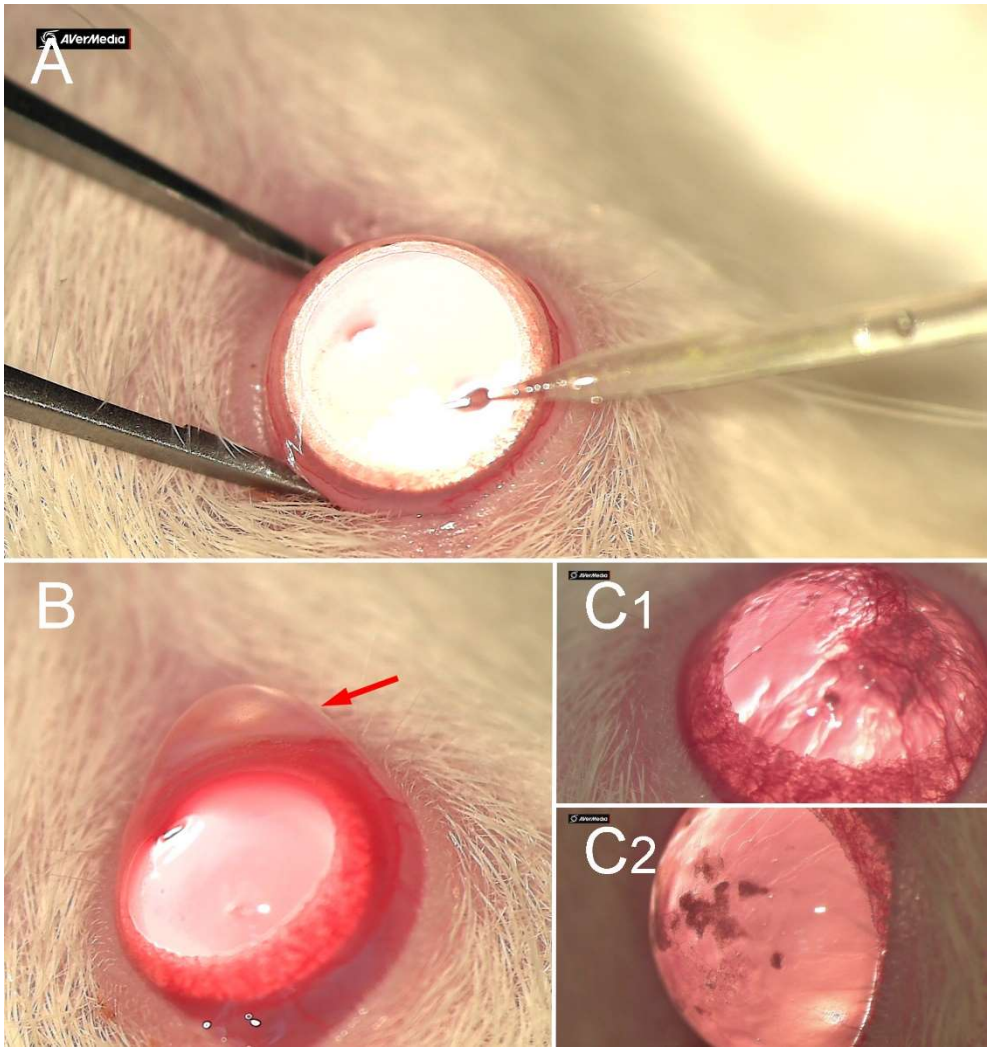

Figure 10. Disadvantage of microbead injection. (**A**) Microbead injection is performed in the same manner as is magnetic bead injection. (**B**) Upon needle removal, microbeads are regurgitated out (red arrow) through a patent needle track due to the high-pressure gradient. Such reflux spillage necessitates injection of larger volumes with repetition, which provokes anterior segment inflammation (**C**). Although the inflammation subsided at postoperative 4 weeks (**C_2**) relative to postoperative 2 weeks (**C_1**), the microbead injection model is less ideal as a rodent glaucoma model than is the magnetic bead injection model.

The magnetic bead injection model effected two gross anatomical changes. First, the steady IOP increase induced apparent buphthalmos in all BN rats and in some of the SD rats. In fact, global eyeball expansion after magnetic bead injection in BN rats has been reported.[32] As occurs in congenital glaucoma, eyeball expansion might be possible under conditions of elastic sclera and steady IOP increase.[32, 44, 45] Although less evident, buphthalmos also was observed in the present study's SD rats. Its lesser occurrence in SD rats might be associated with poorer maintenance of IOP increase with the magnetic bead injection model. As for the second gross anatomical change effected by the magnetic bead injection model, it, unlike the other two models, induced neovascular complications including iris neovascularization and hyphema, though rarely. In our pilot study, the larger magnetic bead injection volume could enable better IOP maintenance from the immediate-postoperative period, but it also led to greater chances of neovascular complications. Therefore, we should limit the injected magnetic bead volume for steady IOP increase. Contrastingly, no neovascular complication was observed in the hydrogel injection or circumlimbal suture models, despite much higher IOP spikes in the immediate-postoperative period. Thus, we speculated, as Tribble et al. did,[32] that magnetic bead injection itself might induce vascular compromise. Although non-toxicity of intracameral magnetic bead injection has been reported for ocular structures,[46] direct toxicity has been noted for endothelial cells.[47] Furthermore, magnetic beads, especially in small particle sizes (4.0–4.9 μm), might surpass the damaged blood-retinal barrier and induce vascular obstruction directly.

In the hydrogel injection model, aqueous humor outflow was blocked by the hydrogel, which had been transformed to the gel state after its injection. Since the

pre-mixed agent was injected in the liquid state, no needle blockage by the injected particles could occur, which allowed for the use of a very fine glass needle tip. Consequently, reflux was minimized, even to the extent that enabled immediate-postoperative IOP spikes. Further, the anterior segment of the eye was unaffected by the particles, due to the transparency of the gel material (**Figure 4**). This certainly would be a great advantage in terms of postoperative imaging. Disadvantageously, however, the IOP increase could not be maintained for more than 2 weeks without a booster injection. This was the reason for having to set a very high immediate-postoperative IOP to maintain IOP elevation longer. Since eyeball expansion was rarely observed, we speculated that this model might simulate subacute IOP elevation model better than chronic glaucoma. Insufficient IOP elevation in the hydrogel model, however, should be interpreted with caution. Our hydrogel model had less IOP elevation when compared to the reference work of Huang et al.[34] Later, Yu et al. showed not only IOP elevation but also functional impairments, which were reversed after IOP-lowering treatments in the hydrogel injection model using SD rats.[37] Therefore, our hydrogel injection method might need to be optimized further. Moreover, newer hydrogel agents[36, 38, 48] and post-injection modification using UV lights[35, 38] have been developed. Therefore, we speculated that the hydrogel injection model can be further improved in the future.

The circumlimbal suture model also required a very high immediate-postoperative IOP. This IOP elevation had dropped by the next day but remained above the normal range for a month. IOP spikes immediately after suturing has been reported consistently for the circumlimbal suture models.[18-20] This contrasted with the gradual decrease or gradual increase in the hydrogel injection model or magnetic

bead injection model, respectively. Interestingly, no inter-strain difference was observed in this model. Since the SD rats are cheaper than the BN type, the circumlimbal suture model would be beneficial in the aspect of cost relative to the other models. On the other hand, this model resulted in lesser RGC death, which fact is probably related to the poorer maintenance of increased IOP. Considering the IOP profile and the absence of eyeball expansion, we speculated that the circumlimbal suture model might simulate acute IOP elevation better than chronic glaucoma.

We used two IOP parameters: 1) maximum IOP and 2) average integral IOP. When we defined IOP elevation in terms of each value over 20 *mmHg*, all of the glaucoma models resulted in IOP elevation for the majority of cases. In the hydrogel injection and circumlimbal suture models, however, high postoperative IOP spikes dragged the IOP values over 20 *mmHg*, whereas in the magnetic bead injection model, gradual IOP increases moved the IOP values over 20 *mmHg*. Therefore, we speculated that, in our study at least, the magnetic bead injection model might reflect glaucoma more accurately than the other two models, and in a way that cannot be represented by numeric values of IOP parameters.

The internal aqueous outflow blocking approach showed inter-strain difference: increased IOP was maintained better in the BN rats than in the SD type. Similar differential susceptibility according to strains has been reported for mice glaucoma models aiming to obstruct the aqueous humor outflow pathway with microbeads: Cone et al. induced an experimental glaucoma model by injecting microbeads and viscoelastics into C57/BL6, DBA/2J, and CD1 mice, and the smallest extent of IOP elevation was observed in the CD1 mice.[22, 26] Since both SD rats and CD1 mice have white hairs unlike other strains, we speculated that the amount of pigmentation might

affect obstruction at the level of the trabecular meshwork, as observed in pigmentary glaucoma.[49] This might in fact be one clue to the ethnic difference of glaucoma manifestation.[50] Further study is necessary to confirm this speculation.

Host immunologic reaction might be another reason for the susceptibility difference between the internal and external approaches. In contrast to the external approach, intracameral injection of foreign bodies could aggravate inflammation.[27] Further, Kezic et al. showed that anterior chamber cannulation alone could induce microglial activation, while the concomitant IOP elevation led to additional Müller cell activation.[51] Therefore, IOP elevation through the internal aqueous outflow blocking approach may be due in part to inflammatory trabeculitis.[10, 21] Interestingly, the retinal pigment epithelium has been reported to contribute to the immune and inflammatory response of the eye not only via part of the blood-eye barrier preserving the immune-privileged status, but also by being the source and target of inflammatory cytokines.[52] Thus, strains with different pigmentation status may show different immunologic reactions. Although we did not observe any gross anatomical difference in inflammation, the difference between glaucoma models observed in this study could become a cornerstone of a novel immunologic evaluation of glaucoma pathogenesis.[4]

To evaluate glaucomatous damage as a consequence of IOP elevation, we determined the RGC density on retinal flat-mounts. This approach could be improved in two ways. First, regional difference of glaucomatous damage could be evaluted using retinal wholemounts.[43] Second, axonal damage could be evaluated using histology sections across the optic nerve head,[53] which protocol provides not only axonal quantification but also information on non-RGC cells and non-cellular

structures with their interactions. We will consider adopting these strategies in the future.

This study shows different modes of IOP elevation among three rodent glaucoma models and their best-matched strains. As such, it could be a reference for future researchers looking to design their own studies. Some might evaluate how the mechansim of IOP elevation induces RGC death, while others might test experimental anti-glaucoma medications to quantify their effects in the aspects of IOP lowering and RGC preservation. Studies of this type are impossible without first establishing glaucoma animal models. Therefore, we encourage future researchers to seek out our work and replicate our approach for confirmation of our speculation.

This study has several limitations. First, this study evaluated only RGC density as the result of elevated IOP in each glaucoma animal model. Evaluation of other retinal cells (such as bipolar cells or photoreceptors) would have been helpful in order to quantify which model led to more RGC-specific injury and, thereby, was more useful as a glaucoma model. Second, despite our success in demonstrating the different clinical profiles of each glaucoma animal model according to strains, we could not determine the exact reason for such differences. Further study would be required to elucidate the down-stream molecular pathways of each model. Third, variation of RGC density existed among the glaucoma models. This was somewhat inevitable, since we could not control for the exact IOP status of every subject. Further, cases with neovascular complication had to be excluded from the magnetic bead injection model, due to the fact that flat-mounting of the retina was not possible. And since those cases were generally associated with higher IOP, we might have excluded severe cases selectively, and thus leading to underestimation of RGC

deaths in our models. RGC density would be more informative if, in future work, IOP status also could be incorporated into models for comparative purposes. Fourth, our comparison of RGC density was based on cross-sectional data, not longitudinal data, since we had to sacrifice the rats in order to count RGCs on the retinal flat-mounts. *In vivo* real-time evaluation of RGCs and their function would be necessary to elucidate the individual effect of IOP change over time in each glaucoma model in the future. Fifth and finally, we did not compare the IOP-normalizing treatment outcomes according to the models and strains. Given that the ultimate goal of these models is to develop novel human glaucoma treatment strategies, further study on the treatment outcomes of different models and strains based on the conventional treatment would be helpful.

In conclusion, the magnetic bead and hydrogel injection models were affected by strains while the circumlimbal suture model was not. Strains should be considered as an important factor when establishing rodent glaucoma animal models. Our recommendations are as follows: 1) the magnetic bead injection model with BN rats if steady increase of IOP is required as in chronic glaucoma, 2) the hydrogel injection model with BN rats if ocular imaging is planned, and 3) the circumlimbal suture model with either BN or SD rats if acute increase of IOP is required.

REFERENCES

1. Quigley HA, Broman AT. The number of people with glaucoma worldwide in 2010 and 2020. *Br J Ophthalmol* 2006;90:262-267.

2. Tham YC, Li X, Wong TY, et al. Global prevalence of glaucoma and projections of glaucoma burden through 2040: a systematic review and meta-analysis. *Ophthalmology* 2014;121:2081-2090.

3. Flaxman SR, Bourne RRA, Resnikoff S, et al. Global causes of blindness and distance vision impairment 1990-2020: a systematic review and meta-analysis. *Lancet Glob Health* 2017;5:e1221-e1234.

4. Weinreb RN, Khaw PT. Primary open-angle glaucoma. *Lancet* 2004;363:1711-1720.

5. Burgoyne CF. A biomechanical paradigm for axonal insult within the optic nerve head in aging and glaucoma. *Exp Eye Res* 2011;93:120-132.

6. Quigley HA. Glaucoma. *Lancet* 2011;377:1367-1377.

7. Weinreb RN, Aung T, Medeiros FA. The pathophysiology and treatment of glaucoma: a review. *Jama* 2014;311:1901-1911.

8. Quigley HA, Addicks EM. Chronic experimental glaucoma in primates. II. Effect of extended intraocular pressure elevation on optic nerve head and axonal transport. *Invest Ophthalmol Vis Sci* 1980;19:137-152.

9. Quigley HA, Hohman RM. Laser energy levels for trabecular meshwork damage in the primate eye. *Invest Ophthalmol Vis Sci* 1983;24:1305-1307.

10. Weber AJ, Zelenak D. Experimental glaucoma in the primate induced by latex microspheres. *J Neurosci Methods* 2001;111:39-48.

11. Kumar S, Benavente-Perez A, Ablordeppey R, et al. A Robust Microbead Occlusion Model of Glaucoma for the Common Marmoset. *Transl Vis Sci Technol* 2022;11:14.

12. Samuelson DA, Gum GG, Gelatt KN. Ultrastructural changes in the aqueous outflow apparatus of beagles with inherited glaucoma. *Invest Ophthalmol Vis Sci* 1989;30:550-561.

13. Grozdanic SD, Betts DM, Sakaguchi DS, et al. Laser-induced mouse model of chronic ocular hypertension. *Invest Ophthalmol Vis Sci* 2003;44:4337-4346.

14. Nakazawa T, Nakazawa C, Matsubara A, et al. Tumor necrosis factor-alpha mediates oligodendrocyte death and delayed retinal ganglion cell loss in a mouse model of glaucoma. *J Neurosci* 2006;26:12633-12641.

15. McKinnon SJ, Schlamp CL, Nickells RW. Mouse models of retinal ganglion cell death and glaucoma. *Exp Eye Res* 2009;88:816-824.

16. Gross RL, Ji J, Chang P, et al. A mouse model of elevated intraocular pressure: retina and optic nerve findings. *Trans Am Ophthalmol Soc* 2003;101:163-169; discussion 169-171.

17. Ruiz-Ederra J, Verkman AS. Mouse model of sustained elevation in intraocular pressure produced by episcleral vein occlusion. *Exp Eye Res* 2006;82:879-884.

18. Liu HH, Bui BV, Nguyen CT, et al. Chronic ocular hypertension induced by circumlimbal suture in rats. *Invest Ophthalmol Vis Sci* 2015;56:2811-2820.

19. Zhao D, Nguyen CT, Wong VH, et al. Characterization of the Circumlimbal Suture Model of Chronic IOP Elevation in Mice and Assessment of Changes in Gene Expression of Stretch Sensitive Channels. *Front Neurosci* 2017;11:41.

20. Lee SH, Sim KS, Kim CY, Park TK. Transduction Pattern of AAVs in the Trabecular Meshwork and Anterior-Segment Structures in a Rat Model of Ocular Hypertension. *Mol Ther Methods Clin Dev* 2019;14:197-205.

21. Urcola JH, Hernandez M, Vecino E. Three experimental glaucoma models in rats: comparison of the effects of intraocular pressure elevation on retinal ganglion cell size and death. *Exp Eye Res* 2006;83:429-437.

22. Cone FE, Gelman SE, Son JL, et al. Differential susceptibility to experimental glaucoma among 3 mouse strains using bead and viscoelastic injection. *Exp Eye Res* 2010;91:415-424.

23. Sappington RM, Carlson BJ, Crish SD, Calkins DJ. The microbead occlusion model: a paradigm for induced ocular hypertension in rats and mice. *Invest Ophthalmol Vis Sci* 2010;51:207-216.

24. Chen H, Wei X, Cho KS, et al. Optic neuropathy due to microbead-induced elevated intraocular pressure in the mouse. *Invest Ophthalmol Vis Sci* 2011;52:36-44.

25. Samsel PA, Kisiswa L, Erichsen JT, et al. A novel method for the induction of experimental glaucoma using magnetic microspheres. *Invest Ophthalmol Vis Sci* 2011;52:1671-1675.

26. Cone FE, Steinhart MR, Oglesby EN, et al. The effects of anesthesia, mouse strain and age on intraocular pressure and an improved murine model of experimental glaucoma. *Exp Eye Res* 2012;99:27-35.

27. Rho S, Park I, Seong GJ, et al. Chronic ocular hypertensive rat model using microbead injection: comparison of polyurethane, polymethylmethacrylate, silica and polystyene microbeads. *Curr Eye Res* 2014;39:917-927.

28. Morgan JE, Tribble JR. Microbead models in glaucoma. *Exp Eye Res* 2015;141:9-14.

29. Ito YA, Belforte N, Cueva Vargas JL, Di Polo A. A Magnetic Microbead Occlusion Model to Induce Ocular Hypertension-Dependent Glaucoma in Mice. *J Vis Exp* 2016:e53731.

30. Biswas S, Wan KH. Review of rodent hypertensive glaucoma models. *Acta Ophthalmol* 2019;97:e331-e340.

31. Calkins DJ, Lambert WS, Formichella CR, et al. The Microbead Occlusion Model of Ocular Hypertension in Mice. *Methods Mol Biol* 2018;1695:23-39.

32. Tribble JR, Otmani A, Kokkali E, et al. Retinal Ganglion Cell Degeneration in a Rat Magnetic Bead Model of Ocular Hypertensive Glaucoma. *Translational Vision Science & Technology* 2021;10:21-21.

33. Chen J, Sun J, Yu H, et al. Evaluation of the Effectiveness of a Chronic Ocular Hypertension Mouse Model Induced by Intracameral Injection of Cross-Linking Hydrogel. *Front Med (Lausanne)* 2021;8:643402.

34. Huang S, Huang P, Liu X, et al. Relevant variations and neuroprotecive effect of hydrogen sulfide in a rat glaucoma model. *Neuroscience* 2017;341:27-41.

35. Guo C, Qu X, Rangaswamy N, et al. A murine glaucoma model induced by rapid in vivo photopolymerization of hyaluronic acid glycidyl methacrylate. *PLoS One* 2018;13:e0196529.

36. Chan KC, Yu Y, Ng SH, et al. Intracameral injection of a chemically cross-linked hydrogel to study chronic neurodegeneration in glaucoma. *Acta Biomater* 2019;94:219-231.

37. Yu H, Zhong H, Chen J, et al. Efficacy, Drug Sensitivity, and Safety of a

Chronic Ocular Hypertension Rat Model Established Using a Single Intracameral Injection of Hydrogel into the Anterior Chamber. *Med Sci Monit* 2020;26:e925852.

38. Kim YK, Kim SN, Min CH, et al. Novel glaucoma model in rats using photo-crosslinked azidobenzoic acid-modified chitosan. *Mater Sci Eng C Mater Biol Appl* 2021;125:112112.

39. Wang WH, Millar JC, Pang IH, et al. Noninvasive measurement of rodent intraocular pressure with a rebound tonometer. *Invest Ophthalmol Vis Sci* 2005;46:4617-4621.

40. Chauhan BC, Pan J, Archibald ML, et al. Effect of intraocular pressure on optic disc topography, electroretinography, and axonal loss in a chronic pressure-induced rat model of optic nerve damage. *Invest Ophthalmol Vis Sci* 2002;43:2969-2976.

41. Cone FE, Steinhart MR, Oglesby EN, et al. The effects of anesthesia, mouse strain and age on intraocular pressure and an improved murine model of experimental glaucoma. *Exp Eye Res* 2012;99:27-35.

42. Frankfort BJ, Khan AK, Tse DY, et al. Elevated intraocular pressure causes inner retinal dysfunction before cell loss in a mouse model of experimental glaucoma. *Invest Ophthalmol Vis Sci* 2013;54:762-770.

43. Guymer C, Damp L, Chidlow G, et al. Software for Quantifying and Batch Processing Images of Brn3a and RBPMS Immunolabelled Retinal Ganglion Cells in Retinal Wholemounts. *Transl Vis Sci Technol* 2020;9:28.

44. Terraciano AJ, Sidoti PA. Management of refractory glaucoma in childhood. *Curr Opin Ophthalmol* 2002;13:97-102.

45. Stowell C, Burgoyne CF, Tamm ER, Ethier CR. Biomechanical aspects of

axonal damage in glaucoma: A brief review. *Exp Eye Res* 2017;157:13-19.

46. Raju HB, Hu Y, Vedula A, Dubovy SR, Goldberg JL. Evaluation of Magnetic Micro- and Nanoparticle Toxicity to Ocular Tissues. *PLOS ONE* 2011;6:e17452.

47. Tiwari A, Punshon G, Kidane A, Hamilton G, Seifalian AM. Magnetic beads (Dynabead™) toxicity to endothelial cells at high bead concentration: Implication for tissue engineering of vascular prosthesis. *Cell Biology and Toxicology* 2003;19:265-272.

48. Liu Y, Wang J, Jin X, et al. A novel rat model of ocular hypertension by a single intracameral injection of cross-linked hyaluronic acid hydrogel (Healaflow(®)). *Basic Clin Pharmacol Toxicol* 2020;127:361-370.

49. Okafor K, Vinod K, Gedde SJ. Update on pigment dispersion syndrome and pigmentary glaucoma. *Curr Opin Ophthalmol* 2017;28:154-160.

50. Gracitelli CPB, Zangwill LM, Diniz-Filho A, et al. Detection of Glaucoma Progression in Individuals of African Descent Compared With Those of European Descent. *JAMA Ophthalmol* 2018;136:329-335.

51. Kezic JM, Chrysostomou V, Trounce IA, et al. Effect of anterior chamber cannulation and acute IOP elevation on retinal macrophages in the adult mouse. *Invest Ophthalmol Vis Sci* 2013;54:3028-3036.

52. Holtkamp GM, Kijlstra A, Peek R, de Vos AF. Retinal Pigment Epithelium-immune System Interactions: Cytokine Production and Cytokine-induced Changes. *Progress in Retinal and Eye Research* 2001;20:29-48.

53. Ebneter A, Casson RJ, Wood JP, Chidlow G. Estimation of axon counts in a rat model of glaucoma: comparison of fixed-pattern sampling with targeted

sampling. *Clinical & Experimental Ophthalmology* 2012;40:626-633.

국문 초록

목적: 세가지 종류의 설치류 녹내장 동물 모델 (전방각 마그네틱 비드 주입 모델, 전방각 하이드로젤 주입 모델, 윤부결막 봉합 모델)에 대해 동물주의 차이가 미치는 영향을 비고하고자 한다.

연구 방법: Brown Norway (BN) rat과 Sprague Dawley (SD) rat에 대해 전방각에 마그네틱 비드 혹은 하이드로젤을 주입하여 방수 유출로를 폐쇄하거나 윤부결막을 봉합을 통한 외부 압박으로 안압 상승을 유발한다. 최대 안압과 시술 이후 1달까지 관찰기간동안 평균 안압을 녹내장 유발 모델 간, 동물주 간 비교한다. 망막신경절세포 사멸을 비교하기 위해 시술 2주와 4주차에 안락사 하여 망막조직을 염색하여 공초점 레이저 주사 현미경을 이용하여 촬영 후 세포 밀도를 분석한다.

결과: 전방각 마그네틱 비드 주입 모델은 점진적인 안압 상승을 보인 반면 전방각 하이드로젤 주입 모델과 윤부결막 봉합 모델은 급격한 안압 상승을 유발하였으며 전방각 하이드로젤 주입 모델의 안압은 서서히, 윤부결막 봉합 모델은 급격한 안압 하강이 관찰되었다. 시술 후 최대 안압은 전방각 하이드로젤 주입 모델과 윤부결막 봉합 모델에서 전방각 마그네틱 비드 주입 모델에서보다 더 높았으나 ($P < 0.001$), 평균 안압은 두 동물주에서 모두 차이를 보이지 않았다 (both $P \geq 0.05$). 일반화 추정 방정식을 이용하여 안압 상승 경과를 비교해 보면 안압 상승은 BN rat에서 SD rat 보다 더 잘 유지되었고 ($P < 0.001$), 그러한 동물주 간 차

이는 윤부결막 봉합 모델에서는 작았다. 시술 후 1달째에 BN rat의 모든 모델에서 유의한 망막 신경절 세포 밀도 감소를 확인할 수 있었던 반면 SD rat에서는 윤부결막 봉합 모델에서만 유의한 감소를 확인할 수 있었다.

결론: BN rat은 전방각 마그네틱 비드 주입 혹은 전방각 하이드로젤 주입을 통하여 방수 유출 경로를 폐쇄하는 모델에 유용한 반면 윤부결막 봉합 모델은 BN rat과 SD rat 모두 비슷한 결과를 보였다. 이처럼 모델 간 안압 상승 및 녹내장 유발 정도가 다르므로 모델 확립 시 동물 주가 미치는 차이를 고려해야 한다.

주요어: 설치류 녹내장 유발 동물 모델; 마그네틱 비드; 하이드로젤; 윤부결막 봉합; 망막 신경절 세포; 안압

학번: 2016-30587